nature neuroscience

Spontaneous fluctuations in neural responses to heartbeats predict visual detection

Hyeong-Dong Park[1], Stéphanie Correia[1], Antoine Ducorps[2] & Catherine Tallon-Baudry[1]

Spontaneous fluctuations of ongoing neural activity substantially affect sensory and cognitive performance. Because bodily signals are constantly relayed up to the neocortex, neural responses to bodily signals are likely to shape ongoing activity. Here, using magnetoencephalography, we show that in humans, neural events locked to heartbeats before stimulus onset predict the detection of a faint visual grating in the posterior right inferior parietal lobule and the ventral anterior cingulate cortex, two regions that have multiple functional correlates and that belong to the same resting-state network. Neither fluctuations in measured bodily parameters nor overall cortical excitability could account for this finding. Neural events locked to heartbeats therefore shape visual conscious experience, potentially by contributing to the neural maps of the organism that might underlie subjectivity. Beyond conscious vision, our results show that neural events locked to a basic physiological input such as heartbeats underlie behaviorally relevant differential activation in multifunctional cortical areas.

Ongoing large-scale neural activity is no longer considered noise but rather a highly structured activity that can shape stimulus-evoked neural responses[1–6] and perceptual performance[7–11]. The structure of large-scale ongoing activity depends on a number of parameters such as anatomical connectivity, intrinsic dynamics and unconstrained mental processes, potentially including self-oriented thoughts[12,13]. Brain-body interactions may constitute another source of spontaneous fluctuations of large-scale brain dynamics. Indeed, the brain is constantly involved in the monitoring and regulation of a number of bodily processes, ranging from proprioceptive information[14] to homeostatic processes involving internal organs such as the heart, gut or lungs[15–18]. Homeostatic regulation relies on not only a reflex loop involving the brainstem but also an additional loop encompassing cortical regions that could influence emotional and cognitive functions[15–19]. Those pervasive ongoing homeostatic processes engaging cortical structures correlate with spontaneous fluctuations of large-scale neural activity. For instance, both activation and connectivity in the default-mode network correlate with ongoing modulations in skin conductance[20–22] or heart rate[23,24]. It is therefore known that ongoing large-scale activity is related to brain-body interactions and that prestimulus ongoing large-scale activity affects stimulus detection. What remains unknown is whether spontaneous fluctuations in brain-body interactions before stimulus onset directly affect stimulus detection.

We tested this hypothesis by measuring neural events locked to heartbeats using magnetoencephalography (MEG) in a visual detection task. Neural activities evoked by heartbeats are obtained by averaging scalp[25,26] or intracranial[27] electrophysiological signals that are time locked to heartbeats to generate the heartbeat-evoked response. Heartbeat-evoked responses are a marker of the cortical representation of cardiac information[25,26], and their amplitudes correlate with interoceptive and empathy abilities[28,29]. At each heartbeat, mechanosensory receptors in the heart and aortic walls transiently discharge at specific phases of the cardiac cycle[30]. This information can be relayed up to the neocortex, with ascending anatomical pathways targeting numerous cortical structures, including the posterior insula[15], ventral anterior cingulate cortex (vACC)[30,31], amygdala[15,16] and somatosensory cortex[27]. Here we show that the successful detection of a visual grating at threshold is predicted by enhanced heartbeat-evoked responses before stimulus onset in vACC and the right inferior parietal lobule without any simultaneous change in a number of bodily physiological parameters or cortical excitability.

RESULTS

Behavior and heart rate modulations

We presented 17 participants with visual stimuli at the threshold for conscious detection while recording both MEG and electrocardiogram (EKG) data (**Fig. 1**). When subjects properly fixated on the center of the screen, a warning stimulus was delivered, and after a variable delay, a faintly contrasted grating annulus was briefly presented in 87% of the trials. After another variable delay, subjects were prompted to report whether or not they saw a stimulus. Stimulus contrast was titrated for each subject in a separate staircase procedure and maintained constant throughout the recordings. Subjects perceived on average 46.4 ± 2.9% (mean ± s.e.m.) of the stimuli while maintaining a low level of false alarms (2.6 ± 0.9%), corresponding to a mean sensitivity, d', of 2.0 ± 0.15 and a decision bias, log(β), of 2.28 ± 0.21. Reaction times were significantly shorter when subjects reported seeing the stimulus (hits: 1,087 ± 37 ms; misses: 1,252 ± 50 ms; paired t test, $t_{16} = 6.6$, $P = 6.10^{-6}$). Hit rate, reaction times, detection sensitivity and decision criterion did not differ between the diastole and systole (**Supplementary Table 1**).

[1]Cognitive Neuroscience Laboratory, Institut National de la Santé et de la Recherche Médicale (INSERM)–École Normale Supérieure (ENS), Paris, France. [2]Cenir, Centre National de la Recherche Scientifique (CNRS)–Université Pierre-et-Marie-Curie (UPMC)-INSERM, Paris, France. Correspondence should be addressed to C.T.-B. (catherine.tallon-baudry@ens.fr).

Received 18 November 2013; accepted 5 February 2014; published online 9 March 2014; doi:10.1038/nn.3671

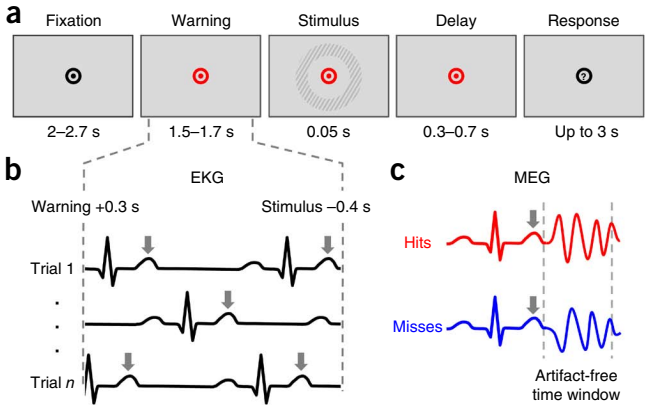

Figure 1 Experimental paradigm and rationale. (**a**) Time course of a target-present trial. Subjects reported whether or not they saw a faint grating annulus. (**b**) Cardiac T waves (arrows) occurring between warning and stimulus onset and detected in single trials in the electrocardiogram. (**c**) Averaged MEG evoked fields locked on the T wave of the electrocardiogram (arrows) to test whether prestimulus neural events locked to heartbeats differed between hits and misses. The analysis focused on the time window free from cardiac artifact during the heart relaxation period after the T wave.

Before measuring neural events locked to heartbeats, we first tested whether heart rate itself distinguished between hits and misses. We measured the mean duration of the interbeat interval during which the warning cue appeared, during which the stimulus appeared or during which subjects responded (**Fig. 2**). Phasic heart rate changes within the course of a trial were revealed by Greenhouse-Geisser–corrected two-way repeated-measure analysis of variance (ANOVA) on interbeat intervals computed at different moments in a trial (factor, time) separately in hits and misses (factor, consciousness). After the warning stimulus appeared on the screen, subjects' hearts slowed down, a phenomenon known as anticipatory cardiac deceleration[32], and accelerated again after subjects gave their response (main effect of time, $F_{1.45,23.15} = 23.2$, $P = 10^{-5}$; *post-hoc* Bonferroni-corrected paired t test, interbeat interval during warning compared to stimulus, $t_{16} = 5.59$, $P = 4.10^{-4}$; response compared to the first interbeat interval after response, R+1, $t_{16} = 5.98$, $P = 2.10^{-4}$). In addition to this overall modulation of heart rate within a trial, consciously seeing the stimulus induced a further slowing down of the heart (main effect of consciousness, $F_{1,16} = 8.5$, $P = 0.01$; time × consciousness interaction, $F_{1.87,30.0} = 3.6$, $P = 0.04$), with a lengthening of interbeat intervals in hits after subjects delivered their response (*post-hoc* Bonferroni-corrected paired t test, hits compared to misses; interbeat interval R+1 after response delivery: $t_{16} = 3.6$, $P = 0.012$; R+2: $t_{16} = 3.6$, $P = 0.012$). Interbeat interval variability also evolved during the course of a trial (**Supplementary Fig. 1**), with a reduction of variability after stimulus presentation, but did not differ between hits and misses. To summarize, before stimulus onset, neither heart rate nor heart rate variability predicted detection, whereas after subjects pressed the button to indicate their response, heart rates were slower in hits.

Heartbeat-evoked responses predict visual detection

We tested the hypothesis that heartbeat-evoked response amplitude before stimulus onset predicted whether the upcoming visual stimulus would be reported as seen. After the decay of the EKG T wave, during the heart relaxation period, responses to heartbeats are free from electrical artifacts due to heart contractions[26,33]. We therefore detected heartbeats occurring during the warning interval preceding stimulus onset, averaged the MEG data locked on the EKG T wave separately in hits and misses (**Fig. 1b**,**c**) and submitted the artifact-free 50–350 ms post–T wave time window to a cluster-based permutation t test. Prestimulus heartbeat-evoked responses significantly differed between hits and misses (Monte-Carlo $P = 0.034$ corrected for multiple comparisons in space and time) over the right frontal and central magnetometers between 135 and 171 ms (**Fig. 3a**,**b**). Effect size was in the typical range of differential cortical responses as measured with MEG, around 10 fT. The hit compared to miss difference in neural events locked to heartbeats corresponded to spontaneous fluctuations around a mean reference level of the neural event locked to heartbeats obtained in a separate resting condition with eyes open in the same subjects (**Fig. 3c**): heartbeat-evoked responses during rest were smaller than in hits (paired t test, $t_{16} = 2.8$, $P = 0.013$) but were larger than in misses (paired t test, $t_{16} = 2.4$, $P = 0.029$). Heartbeat-evoked responses distinguished between hits and misses both at the beginning ($t_{16} = 4.1$, $P = 8.10^{-4}$) and end ($t_{16} = 3.0$, $P = 8.10^{-3}$; median split of the latency of heartbeats with respect to stimulus onset) of the warning interval. The effect was significant in both subjects with fast heart rate ($P = 0.006$) and subjects with slow heart rate ($P = 0.015$) at similar latencies (**Supplementary Fig. 2**). Heartbeat-evoked neural responses preceding correct rejections were significantly smaller than responses preceding hits ($t_{16} = 2.95$, $P = 0.009$) and were not different from responses preceding misses ($t_{16} = 1.40$, $P = 0.18$).

We then tested directly whether neural events locked to heartbeats were predictive of perception. In each subject, we sorted single trials according to the amplitude of the heartbeat-evoked response (mean magnetometer amplitude across the cluster in the 135–171 ms time window) and organized them into three equally sized bins (averaging 165 ± 8 trials per bin and per subject; min 111, max 229) from low to high amplitude. For each subject, we then computed in each bin

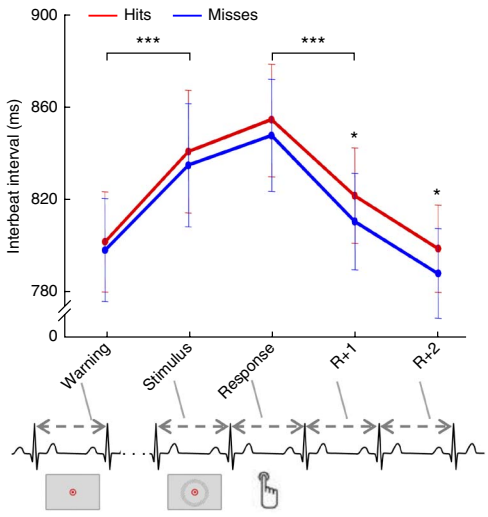

Figure 2 Post-decisional heart slowing. Evolution of the mean interval between R peaks in hits and misses during a trial from the interbeat interval during which the warning cue appeared on the screen (warning) until the interbeat interval during which subjects responded (response) and intervals after the response (R+1 and R+2). Before stimulus onset, heart rate did not distinguish between hits and misses. In all trials, the heart slowed down after warning and accelerated after response delivery. Consciously seeing the stimulus further slowed down the heart, especially after subjects pressed the button to signal their decision (*post hoc* Bonferroni-corrected paired t test between hits and misses, R+1 $t_{16} = 3.6$, $P = 0.012$; R+2 $t_{16} = 3.6$, $P = 0.012$). Error bars represent the s.e.m. $^*P < 0.05$, $^{***}P < 0.0005$, *post hoc* Bonferroni-corrected t test ($n = 17$).

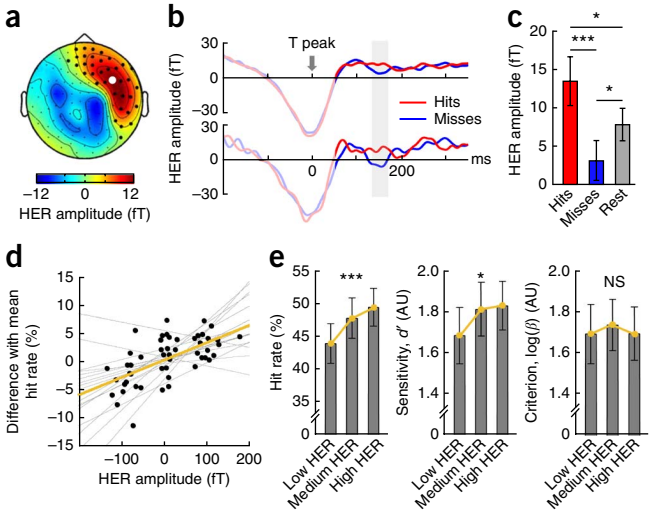

Figure 3 Neural events locked to heartbeats before stimulus onset predicted conscious perception of the stimulus. (**a**) Topographical map of the heartbeat-evoked response (HER) difference between hits and misses grand averaged across 17 subjects in the 135–171 ms time window in which a significant difference was observed (Monte-Carlo $P = 0.034$ corrected for multiple comparisons in time and space) on magnetometer sensors. Larger black dots indicate the location of the magnetometers contributing to the significant cluster. (**b**) Prestimulus T-locked evoked magnetic fields averaged across the cluster (top) and at the sensor indicated by a white dot in **a** (bottom). The signal that was contaminated by the cardiac artifact, before +50 ms, appears in lighter color. The shaded area highlights the time window in which a significant difference was observed. (**c**) Amplitude of the prestimulus HER averaged across the cluster in the 135–171 ms time window in hits and misses and during a separate resting session with eyes open. HERs during rest were smaller than those preceding hits ($P = 0.013$) and larger than those preceding misses ($P = 0.029$, paired t tests; $n = 17$). (**d**) Perceptual performance as a function of prestimulus neural response to heartbeats. In each subject, we sorted single trials in three bins according to the amplitude of the neural response to heartbeats. Each dot corresponds to the mean amplitude in a given bin and in a given subject. When the neural response to heartbeats was larger, subjects were more likely to report seeing the stimulus. Thin gray lines represent the slope of the linear regression between change in hit rate and neural amplitude in each subject. The yellow line indicates the mean slope of the linear regression averaged across subjects. (**e**) The linear increase in hit rate (linear trend analysis; $n = 17$) with increasing HER amplitude (left) corresponded to an increase in sensitivity (middle; $P = 0.049$) without change in criterion (right; $P = 0.99$). AU, arbitrary units. Error bars represent the s.e.m. $^*P < 0.05$, $^{***}P < 0.0005$. NS, not significant.

the change in hit rate relative to the subject's mean hit rate computed across all trials and computed the linear regression between neural amplitude and hit rate change (**Fig. 3d**). Across subjects, both Pearson correlation coefficients and slope values were significantly larger than 0 (mean r, 0.65 ± 0.13; t test against 0, $t_{16} = 5.02$, $P = 10^{-4}$; mean slope, 0.0308 ± 0.007; $t_{16} = 4.61$, $P = 3.10^{-4}$). The increase in hit rate with increasing heartbeat-evoked response amplitude (linear trend analysis, $F_{1,16} = 19.8$, $P = 4.10^{-4}$) was associated with an increased sensitivity ($F_{1,16} = 4.53$, $P = 0.049$) without a change in criterion ($F_{1,16} = 0$, $P = 0.99$) (**Fig. 3e**).

Neural sources of differential responses to heartbeats

To uncover the cortical regions contributing to the differential responses to prestimulus heartbeats in hits and misses identified at the sensor level, we reconstructed the neural sources of MEG activity separately in hits and misses. Two regions were consistently differentially activated (**Fig. 4a** and **Table 1**): one extending across the vACC and ventromedial prefrontal cortex bilaterally (vACC-vmPFC), a region that is known to receive cardiac inputs from subcortical relays[30,31], and another in the posterior part of right inferior parietal lobule (rIPL) in the angular gyrus. Both of these regions of interest survived multiple comparison correction (clustering procedure across all cortical vertices on the mean 135–171 ms currents, both regions with Monte-Carlo $P < 0.05$). We observed an additional differential response to heartbeats in the right midposterior insula (**Table 1**), which is a known cortical target of heartbeat-related afferent signals[15], but this region did not survive multiple comparison correction. The time course of reconstructed neural currents (**Fig. 4b**) confirms that the difference between hits and misses corresponds to an enhanced neural event locked to heartbeats in hits. It further suggests that the effect is initiated in vACC-vmPFC, which is then followed in the posterior rIPL by a transient response to heartbeats appearing only in hits.

Notably, the strength of the differential response to heartbeats before stimulus onset in vACC-vmPFC predicted the post-decisional slowing down of the heart observed 2–3 s later (difference between hits and misses of the mean interbeat interval in the R+2 interval as a function of the difference between hits and misses of the mean 135–171 ms currents in vACC-vmPFC, Pearson's correlation, $r = 0.65$, $P = 0.005$) (**Fig. 4c**). This effect is consistent with the known role of vACC-vmPFC on autonomic control[34]. The differential response to heartbeats before stimulus onset in the posterior rIPL did not correlate significantly with post-stimulus heart slowing ($r = 0.42$, $P = 0.09$).

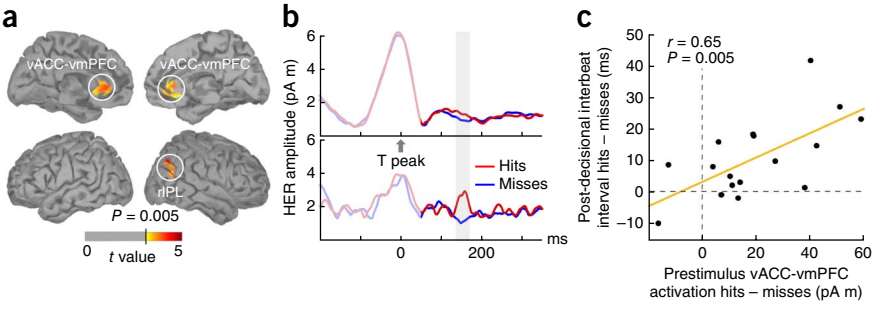

Figure 4 Neural sources of the differential response to heartbeats. (**a**) Differential activation by heartbeats in vACC-vmPFC bilaterally and rIPL in hits and misses before stimulus onset (criterion for visualization purpose, more than ten contiguous vertices with uncorrected $P < 0.005$, paired t test; $n = 17$). (**b**) Time course of the HER in vACC-vmPFC (top) and rIPL (bottom) separately in hits and misses grand averaged across subjects in absolute values of dipole currents (pA m), directly reflecting neural electrical activity. Signal that was contaminated by the cardiac artifact, before +50 ms, appears in lighter color. The shaded area highlights the time window in which we observed a significant difference (clustering procedure at the sensor level; $n = 17$). A larger neural response to heartbeats in hits occurred in both areas, with a more transient effect in rIPL than in vACC-vmPFC. (**c**) Hit-miss difference in cardiac interbeat interval after response delivery as a function of hit-miss difference in HER before stimulus onset in vACC-vmPFC. Each dot represents a subject. These two independent measures were significantly correlated (Pearson $r = 0.65$, $P = 0.005$; $n = 17$).

Table 1 MNI coordinates (mm) of prestimulus differential heartbeat-evoked responses

Region	x	y	z	Cluster size (cm^2)	Anatomical description
Posterior rIPL	52	−67	28	3.67	Angular gyrus, extending ventrally into the dorsal part of the middle temporal gyrus
Left vACC-vmPFC	−3	36	−4	5.00	Anterior cingulate
Right vACC-vmPFC	4	37	−6	3.26	Anterior cingulate, extending ventrally into the dorsal part of the frontal medial orbital region
Right midposterior insula	38	−12	15	0.92	Insula

The differential effect in the midposterior insula did not survive correction for multiple comparisons. MNI, Montreal Neurological Institute.

Controls for volume conduction effect

We checked that the differential response to heartbeats observed on MEG sensors was not due to differences in cardiac electrical activity *per se* directly affecting MEG data by volume conduction, even if the time window analyzed (50–350 ms after the T peak) is known to be free from cardiac artifact[26,33]. We recorded EKG signals from seven electrodes around the base of the neck to carefully monitor the potential direct contribution of heart electrical activity to MEG signals[26]. The EKG data appeared similar in hits and misses (**Supplementary Fig. 3**), on both vertical and horizontal derivations computed offline as bipolar derivations between adjacent electrodes. We submitted EKG signals to the same cluster-based permutation *t* test as the MEG data and found no differences between hits and misses (vertical EKG: smallest Monte-Carlo $P = 0.52$; horizontal EKG: smallest Monte-Carlo $P = 0.17$). Correcting the MEG data for the cardiac artifact using a standard independent component analysis procedure did not affect the results (**Supplementary Fig. 4**).

We also checked that EKG was more sensitive to heart electrical activity than MEG by measuring for each subject the signal-to-noise ratio on the EKG lead and on the magnetometer showing the largest amplitude at T-wave latency (signal-to-noise ratio, EKG: 8.4 ± 3.8; MEG: 0.7 ± 0.3; paired *t* test, $t_{16} = 8.5$, $P = 2.10^{-7}$). For all these reasons, the difference in heart-evoked response between hits and misses observed on MEG sensors cannot be attributed to differences in cardiac electrical activity.

The effect is time locked to the preceding heartbeat

Is the observed difference on MEG signals truly locked to heartbeats, or does it reflect some sustained prestimulus fluctuations of neural activity not specifically linked to heartbeats, for instance, a slow wave developing during the warning interval? We first checked that the latency distribution of the T peaks during the warning interval was similar in hits and misses (density of T peaks in 50-ms time bins, two-way ANOVA with factors time bin and trial type, no main effect of trial type or interaction between time bin and trial type, both $P > 0.4$). To further show that the effect is locked to heartbeats, we created for each subject surrogate heartbeats with the same mean rate and same interbeat interval as the original data but occurring at randomized latencies during the warning interval. We then computed neural responses locked to those surrogate heartbeats during the warning interval separately in hits and misses in each subject, computed the largest cluster *t* statistic across subjects and repeated the whole procedure 100 times. We never found cluster statistics equal to or greater than the one initially obtained on neural data averaged with respect to real heartbeats, thereby confirming that the effects described here are significantly locked to heartbeats (Monte-Carlo $P < 0.01$). The latency of the differential activity was similar in subjects with slow or fast heart rate (**Supplementary Fig. 2**), indicating that the effect corresponds to a differential response to the preceding heartbeat rather than to a preparation of the next heartbeat. These control analyses further demonstrate that the differential neural effect described here is locked to the preceding heartbeat.

We also tested whether we could find significant differences between hits and misses on data locked to warning onset. We first ran a multivariate pattern analysis using a linear support vector machine classifier with twofold validation on prestimulus data locked to warning. In none of the subjects did the multivariate pattern analysis perform significantly better than chance (binomial test in each subject, all $P > 0.4$; 55.0 ± 1.5% (mean accuracy ± s.e.m.)). We then considered warning-locked data averaged across trials and ran the clustering test from 300 to 1,500 ms after the warning. No significant cluster could be found (smallest Monte-Carlo $P = 0.40$). We also ran the clustering test on warning-locked averaged fields using 300-ms-long sliding time windows with onsets ranging from 300 to 1,100 ms in 200-ms steps but did not find any significant cluster (all Monte-Carlo $P > 0.1$).

Pupil diameter and cortical excitability

Changes in arousal may induce a change in pupil diameter that could directly affect visual detection at threshold. However, pupil diameter did not differ between hits and misses (mean pupil diameter during the 1.5 s preceding stimulus onset, arbitrary units, hits: 2.13 ± 0.13; misses: 2.17 ± 0.69; paired *t* test, $t_{16} = 0.24$, $P = 0.82$; **Fig. 5a**).

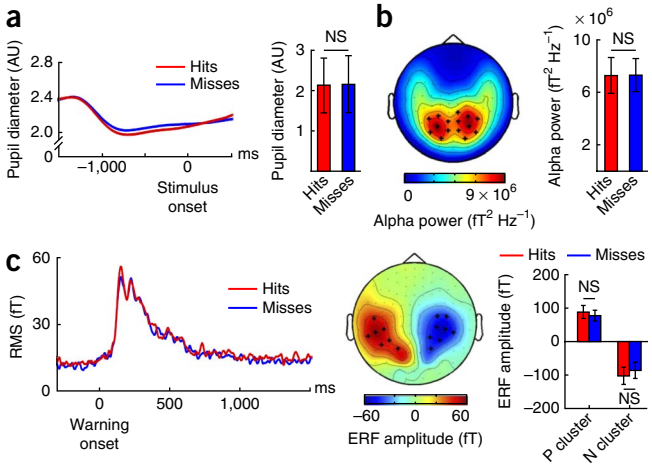

Figure 5 Pupil diameter, alpha power and warning-evoked response do not predict detection ($n = 17$). (**a**) Pupil diameter during the 1.5 s preceding stimulus onset (left, time course; right, mean amplitude) did not predict stimulus detection ($P = 0.82$). (**b**) Alpha power before stimulus onset did not discriminate between hits and misses. Left, topographical map of the mean 1.5 s, 8–12 Hz power with parieto-occipital alpha power averaged over hits and misses. Black crosses indicate sensors with large alpha power. Right, bar graph of the mean alpha power at the sensors marked by crosses on the map separately in hits and misses ($P = 0.94$). (**c**) Neural responses evoked by the warning cue were similar in hits and misses. Left, root mean square (RMS) average across all magnetometers in hits and misses. Middle, topographical map of the most prominent peak of the event-related field (ERF) around 150 ms averaged across subjects and conditions. Black crosses indicate sensors with large responses. Right, bar graph of magnetic field amplitude separately in hits and misses over the sensors showing the largest outgoing positive field ($P = 0.12$) or largest ingoing negative field ($P = 0.11$). Error bars represent the s.e.m.

The differential heartbeat-evoked response could also be due to an overall increase in cortical excitability in hits, a state in which the brain would respond more to any type of input, external or internal. We analyzed alpha power, a marker of cortical excitability, before stimulus onset, but neither a clustering test across all sensors (−1.5 to 0 s, 8–12 Hz, no significant cluster, smallest Monte-Carlo $P = 0.88$) nor a direct comparison between hits and misses on parieto-occipital sensors ($t_{16} = 0.07$, $P = 0.94$) revealed any difference in alpha power before stimulus onset (**Fig. 5b**). In addition, the visual response evoked by the warning cue (**Fig. 5c**) did not differ between hits and misses (clustering test across all sensors on the 0–400 ms after warning onset, no significant cluster, smallest Monte-Carlo $P = 0.28$; direct comparison between hits and misses on the sensors showing the largest evoked response at the peaking latency of global field power: 135–165 ms time window, outgoing positive field, $t_{16} = 1.64$, $P = 0.12$; ingoing negative field, $t_{16} = 1.70$, $P = 0.11$).

Cardiorespiratory parameters

We tested whether a number of cardiorespiratory parameters differed between hits and misses before stimulus onset. Neither heart rate nor heart rate variability measured before stimulus onset differed between hits and misses (**Supplementary Table 2**). We then tested whether hits and misses were characterized by different respiration patterns. The duration of the respiration cycle during which the warning occurred was similar in hits and misses (hits: 3.65 ± 0.17 s; misses: 3.64 ± 0.18 s; paired t test, $t_{16} = 0.06$, $P = 0.95$). At the group level, there was no indication that respiration was locked to stimulus onset, either in hits or in misses (**Supplementary Fig. 5**), and there was no systematic shift in respiration phase between hits and misses (phase bifurcation index between hits and misses, mean $-6.10^{-4} \pm 3.10^{-4}$, not larger than expected by chance, Monte-Carlo $P = 0.63$). No subject showed a significant difference in respiration phase distribution between hits and misses (Kuiper test, Bonferroni corrected, all $P > 0.26$).

We obtained peripheral blood pressure data in a subset of subjects ($n = 11$; **Supplementary Fig. 6**) in arbitrary units. We did not find any prestimulus difference between hits and misses in systolic, diastolic or in the difference between systolic and diastolic pressure (**Supplementary Table 3**), although the prestimulus heartbeat-evoked activity in MEG signals differed between hits and misses in those 11 subjects (hits: 12.9 ± 3.9 fT; misses 4.7 ± 3.2 fT; paired t test, $t_{10} = 2.89$, $P = 0.016$). Throughout the trial, blood pressure did not differ between hits and misses (**Supplementary Fig. 7**).

DISCUSSION

Our results reveal that differential activation locked to heartbeats in vACC-vmPFC and the posterior rIPL before stimulus onset predicts visual detection: when a faint visual stimulus was presented in those states during which the brain responded vigorously to heartbeats, subjects were more likely to perceive the stimulus consciously. Before stimulus onset, neither bodily state nor cortical excitability predicted visual detection. Later on, seeing the stimulus modulated bodily state: the heart slowed down more after subjects reported seeing the stimulus. Post-decisional heart rate slowing correlated with the amplitude of the prestimulus differential response to heartbeats in vACC-vmPFC. These results go beyond previous results showing the importance of brain-body interactions[15,17,18] in several respects. First, the current results apply to the detection of an emotionally neutral and meaningless grating at threshold. Neural responses to heartbeats therefore seem to shape conscious vision in its simplest form. Second, within brain-body interactions, we could separate over time fluctuations of neural activity locked to heartbeats from bodily consequences: fluctuations in neural events locked to heartbeats both preceded and predicted post-decisional heart rate slowing. Third, the differential heartbeat-evoked response took place in vACC and the posterior rIPL. These two structures belong to the same resting-state network and are differentially activated in a large variety of tasks. Our results therefore reveal that a physiological event such as a heartbeat can drive behaviorally relevant activity in coupled multifunctional structures in the absence of concomitant changes in pupil diameter or alpha power as well as in a number of cardiorespiratory parameters.

The effects reported here are consistent with the literature on neural events locked to heartbeats, with anatomical pathways of heart-brain communication and with existing cortical connectivity patterns. First, the prestimulus difference in neural response to heartbeats took place at around 150 ms after the T peak, i.e., about 400 ms after the R peak, which is in keeping with the literature on heart-evoked responses reporting differential responses between 250 and 550 ms after the R peak[27]. Second, we observed a differential response to heartbeats in vACC and the posterior rIPL, two regions whose activity is known to systematically co-fluctuate at rest[35]. vACC is a visceral center, both receiving afferent cardiac information and sending descending commands that regulate heart rate[31]. Of note, we observed another differential heartbeat-locked activation in the insula, a main recipient of visceral information[15], but that region did not survive multiple comparison correction, probably because of the smaller size of the differentially activated cluster in this structure. Third, the effects were not only statistically robust, but they were also internally consistent: the increase in neural response to heartbeats before stimulus onset in vACC-vmPFC predicted the size of the post-decisional slowing down of the heart. Those two variables were obtained from independent measures (source reconstruction of neural responses to heartbeats or heart interbeat intervals) at two different times (before stimulus or after decision).

Before stimulus onset, we observed a neural event locked in time to heartbeats that is predictive of a subject's behavior. Prestimulus effects are often interpreted in terms of changes in alertness or attention. Our results are unlikely to reflect enhanced selective attention toward bodily signals. Indeed, subjects could sometimes pay attention to internal stimuli such as heartbeats and therefore miss external visual stimuli. An interpretation based on selective attention would predict enhanced responses to heartbeats in misses, whereas we observed enhanced responses to heartbeats in hits. In addition, explicitly paying attention to one's own heartbeats[28] alters neural activity in the dorsal ACC, anterior insula and frontal operculum and supplementary motor cortex[36], whereas the effect reported here occurred in vACC-vmPFC and rIPL. Our results also do not seem to reflect fluctuations of tonic alertness (sometimes also called vigilant or sustained attention), as tonic alertness is typically associated with fluctuations of alpha power[37] in a network comprising the dorsal ACC and frontal operculum[38] that were not observed here. The design of our paradigm, with a warning cue triggered by the subject's steady fixation, probably minimized the influence of tonic alertness fluctuations. Additionally, the brain does not seem to be responding more to any type of input in hits, whether internal or external, as the neural response to the warning cue was similar in hits and misses.

The effect reported here was time locked to the preceding heartbeat and can therefore be considered as a neural response to an internal stimulus, the heartbeat. Spontaneous fluctuations in neural responses to heartbeats could have two distinct and nonexclusive origins: variability in ongoing neural dynamics or variability in heartbeat strength. The anatomical location of the differentially activated areas

suggests a contribution of spontaneous fluctuations of default-mode network activity without concomitant changes in occipitoparietal excitability. We could not detect changes in heartbeat strength before stimulus onset within the cardiorespiratory parameters measured (EKG, heart rate, heart rate variability, respiration period and phase and blood pressure). However, we did not measure all cardiorespiratory parameters (for example, stroke volume or respiration volume), and within the measured parameters we may have lacked the sensitivity to detect subtle differences. The respective contributions of cardiac and neural fluctuations to the effect reported here thus remain to be determined.

Larger heartbeat-evoked responses predicted higher hit rate and detection sensitivity without any change in criterion. Heartbeat-evoked responses were larger in hits than in both misses and correct rejections. This pattern of results suggests that heartbeat-evoked responses contribute directly to the signal used for the final perceptual decision. We propose that heartbeat-evoked responses carry information related to the subjective dimension of visual experience[39]. Reporting subjective experience, such as when saying 'I saw the stimulus', is the hallmark of conscious vision[40]. It implies taking a first-person perspective: when reporting seeing consciously, a participant implicitly refers to himself or herself as being the subject experiencing the visual stimulus[19,41]. The ability to say 'I' requires the existence of a biological substrate for the definition of the organism as an entity, a neural referential constituting a subjective frame, from which reporting 'I saw the stimulus' is possible. Neural maps of the state of the organism have been proposed to underlie the emergence of this neural subjective frame using both proprioceptive[14] and visceral information[15,17,18,39], such as heartbeats. Here, larger responses to heartbeats in vACC-vmPFC and rIPL could index a higher level of activity of the neural subjective frame, a signal that would be combined with sensory evidence to produce the report 'I saw the stimulus'. Beyond the present experiment, this interpretation would be in keeping with the known implications of both vACC and the posterior rIPL in a variety of situations engaging subjective experience. The posterior rIPL has been associated, for instance, with perspective taking[42], motor intention[43], self-related judgments[44] and reward evaluation[45]. vACC-vmPFC has been associated with emotion[46], explicit self-related processes[47] and subjective reward value[48]. Part of the anatomical overlap between activations in those seemingly very different studies could correspond to the engagement of subjective experience and enhanced neural responses to heartbeats.

Whether this tentative interpretation in terms of neural subjective frame holds or not, our results indicate that detection performance can be predicted from bodily signal monitoring in vACC-vmPFC and the posterior rIPL. As mentioned above, those two regions can be differentially activated in a wide variety of tasks. The classical approach to characterize the role of multifunctional regions is to search for the most basic psychological process that is common to all the tasks differentially activating such a region[46,49,50]. We propose here to consider the additional framework of physiology: behaviorally relevant differential activation in multifunctional areas can be due to differential neural responses to bodily, physiologically vital inputs. A parcellation of cortical functions in terms of differential physiological responses to bodily signals could be a valuable addition to the more classical attempt at understanding cortical functions in terms of psychological processes.

METHODS

Methods and any associated references are available in the online version of the paper.

Note: Any Supplementary Information and Source Data files are available in the online version of the paper.

ACKNOWLEDGMENTS

This work was supported by Agence Nationale de la Recherche grants ANR-BLAN-12-BSH2-0002-01 to C.T.B., ANR-10-LABX-0087 IEC and ANR-10-IDEX-0001-02 PSL*. We thank E. Koechlin for useful suggestions on the manuscript and C. Gitton for excellent technical support during data acquisition.

AUTHOR CONTRIBUTIONS

H.-D.P. and C.T.-B. designed the experiment. H.-D.P. and S.C. acquired the data. H.-D.P., A.D. and C.T.-B. analyzed the data. H.-D.P. and C.T.-B. wrote the paper.

COMPETING FINANCIAL INTERESTS

The authors declare no competing financial interests.

1. Arieli, A., Sterkin, A., Grinvald, A. & Aertsen, A. Dynamics of ongoing activity: explanation of the large variability in evoked cortical responses. *Science* **273**, 1868–1871 (1996).
2. Greicius, M.D. & Menon, V. Default-mode activity during a passive sensory task: uncoupled from deactivation but impacting activation. *J. Cogn. Neurosci.* **16**, 1484–1492 (2004).
3. Lakatos, P. *et al.* An oscillatory hierarchy controlling neuronal excitability and stimulus processing in the auditory cortex. *J. Neurophysiol.* **94**, 1904–1911 (2005).
4. Poulet, J.F. & Petersen, C.C. Internal brain state regulates membrane potential synchrony in barrel cortex of behaving mice. *Nature* **454**, 881–885 (2008).
5. Marguet, S.L. & Harris, K.D. State-dependent representation of amplitude-modulated noise stimuli in rat auditory cortex. *J. Neurosci.* **31**, 6414–6420 (2011).
6. He, B.J. Spontaneous and task-evoked brain activity negatively interact. *J. Neurosci.* **33**, 4672–4682 (2013).
7. Linkenkaer-Hansen, K., Nikulin, V.V., Palva, S., Ilmoniemi, R.J. & Palva, J.M. Prestimulus oscillations enhance psychophysical performance in humans. *J. Neurosci.* **24**, 10186–10190 (2004).
8. Boly, M. *et al.* Baseline brain activity fluctuations predict somatosensory perception in humans. *Proc. Natl. Acad. Sci. USA* **104**, 12187–12192 (2007).
9. Sadaghiani, S., Hesselmann, G. & Kleinschmidt, A. Distributed and antagonistic contributions of ongoing activity fluctuations to auditory stimulus detection. *J. Neurosci.* **29**, 13410–13417 (2009).
10. Palva, J.M. *et al.* Neuronal long-range temporal correlations and avalanche dynamics are correlated with behavioral scaling laws. *Proc. Natl. Acad. Sci. USA* **110**, 3585–3590 (2013).
11. Vinnik, E., Itskov, P.M. & Balaban, E. Beta- and gamma-band EEG power predicts illusory auditory continuity perception. *J. Neurophysiol.* **108**, 2717–2724 (2012).
12. Fox, M.D. & Raichle, M.E. Spontaneous fluctuations in brain activity observed with functional magnetic resonance imaging. *Nat. Rev. Neurosci.* **8**, 700–711 (2007).
13. Deco, G., Jirsa, V.K. & McIntosh, A.R. Emerging concepts for the dynamical organization of resting-state activity in the brain. *Nat. Rev. Neurosci.* **12**, 43–56 (2011).
14. Blanke, O. Multisensory brain mechanisms of bodily self-consciousness. *Nat. Rev. Neurosci.* **13**, 556–571 (2012).
15. Craig, A.D. How do you feel? Interoception: the sense of the physiological condition of the body. *Nat. Rev. Neurosci.* **3**, 655–666 (2002).
16. Mayer, E.A. Gut feelings: the emerging biology of gut-brain communication. *Nat. Rev. Neurosci.* **12**, 453–466 (2011).
17. Critchley, H.D. & Harrison, N.A. Visceral influences on brain and behavior. *Neuron* **77**, 624–638 (2013).
18. Damasio, A. & Carvalho, G.B. The nature of feelings: evolutionary and neurobiological origins. *Nat. Rev. Neurosci.* **14**, 143–152 (2013).
19. Christoff, K., Cosmelli, D., Legrand, D. & Thompson, E. Specifying the self for cognitive neuroscience. *Trends Cogn. Sci.* **15**, 104–112 (2011).
20. Patterson, J.C. II, Ungerleider, L.G. & Bandettini, P.A. Task-independent functional brain activity correlation with skin conductance changes: an fMRI study. *Neuroimage* **17**, 1797–1806 (2002).
21. Nagai, Y., Critchley, H.D., Featherstone, E., Trimble, M.R. & Dolan, R.J. Activity in ventromedial prefrontal cortex covaries with sympathetic skin conductance level: a physiological account of a "default mode" of brain function. *Neuroimage* **22**, 243–251 (2004).
22. Fan, J. *et al.* Spontaneous brain activity relates to autonomic arousal. *J. Neurosci.* **32**, 11176–11186 (2012).
23. Wong, S.W., Masse, N., Kimmerly, D.S., Menon, R.S. & Shoemaker, J.K. Ventral medial prefrontal cortex and cardiovagal control in conscious humans. *Neuroimage* **35**, 698–708 (2007).
24. Ziegler, G., Dahnke, R., Yeragani, V.K. & Bar, K.J. The relation of ventromedial prefrontal cortex activity and heart rate fluctuations at rest. *Eur. J. Neurosci.* **30**, 2205–2210 (2009).

25. Schandry, R. & Montoya, P. Event-related brain potentials and the processing of cardiac activity. *Biol. Psychol.* **42**, 75–85 (1996).
26. Gray, M.A. *et al.* A cortical potential reflecting cardiac function. *Proc. Natl. Acad. Sci. USA* **104**, 6818–6823 (2007).
27. Kern, M., Aertsen, A., Schulze-Bonhage, A. & Ball, T. Heart cycle-related effects on event-related potentials, spectral power changes, and connectivity patterns in the human ECoG. *Neuroimage* **81**, 178–190 (2013).
28. Montoya, P., Schandry, R. & Muller, A. Heartbeat evoked potentials (HEP): topography and influence of cardiac awareness and focus of attention. *Electroencephalogr. Clin. Neurophysiol.* **88**, 163–172 (1993).
29. Fukushima, H., Terasawa, Y. & Umeda, S. Association between interoception and empathy: evidence from heart-beat evoked brain potential. *Int. J. Psychophysiol.* **79**, 259–265 (2011).
30. Amour, J.A. & Ardell, J.L. *Basic and Clinical Neurocardiology* (Oxford University Press, Oxford, 2004).
31. Vogt, B.A. & Derbyshire, S.W.G. Visceral circuits and cingulate-mediated autonomic functions. in *Cingulate Neurobiology and Disease* (ed. Vogt, B.A.) 220–235 (Oxford University Press, Oxford, 2009).
32. Lacey, B.C. & Lacey, J.I. Studies of heart rate and other bodily processes in sensorimotor behavior. in *Cardiovascular Psychophysiology* (ed. Obrist, P.A., Black, A.H., Brener, J. & DiCara, L.) 538–564 (Aldine Press, Chicago, 1974).
33. Dirlich, G., Dietl, T., Vogl, L. & Strian, F. Topography and morphology of heart action-related EEG potentials. *Electroencephalogr. Clin. Neurophysiol.* **108**, 299–305 (1998).
34. Devinsky, O., Morrell, M.J. & Vogt, B.A. Contributions of anterior cingulate cortex to behaviour. *Brain* **118**, 279–306 (1995).
35. Fox, M.D. *et al.* The human brain is intrinsically organized into dynamic, anticorrelated functional networks. *Proc. Natl. Acad. Sci. USA* **102**, 9673–9678 (2005).
36. Critchley, H.D., Wiens, S., Rotshtein, P., Ohman, A. & Dolan, R.J. Neural systems supporting interoceptive awareness. *Nat. Neurosci.* **7**, 189–195 (2004).
37. Makeig, S. & Inlow, M. Lapses in alertness: coherence of fluctuations in performance and EEG spectrum. *Electroencephalogr. Clin. Neurophysiol.* **86**, 23–35 (1993).
38. Sadaghiani, S. *et al.* Intrinsic connectivity networks, alpha oscillations, and tonic alertness: a simultaneous electroencephalography/functional magnetic resonance imaging study. *J. Neurosci.* **30**, 10243–10250 (2010).
39. Park, H.D. & Tallon-Baudry, C. The neural subjective frame: from bodily signals to perceptual consciousness. *Phil. Trans. R. Soc. B* (in the press).
40. Crick, F. & Koch, C. Towards a neurobiological theory of consciousness. *Semin. Neurosci.* **2**, 263–275 (1990).
41. Vogeley, K. & Fink, G.R. Neural correlates of the first-person-perspective. *Trends Cogn. Sci.* **7**, 38–42 (2003).
42. Ruby, P. & Decety, J. Effect of subjective perspective taking during simulation of action: a PET investigation of agency. *Nat. Neurosci.* **4**, 546–550 (2001).
43. Desmurget, M. *et al.* Movement intention after parietal cortex stimulation in humans. *Science* **324**, 811–813 (2009).
44. Lou, H.C. *et al.* Parietal cortex and representation of the mental Self. *Proc. Natl. Acad. Sci. USA* **101**, 6827–6832 (2004).
45. Fliessbach, K. *et al.* Social comparison affects reward-related brain activity in the human ventral striatum. *Science* **318**, 1305–1308 (2007).
46. Lindquist, K.A., Wager, T.D., Kober, H., Bliss-Moreau, E. & Barrett, L.F. The brain basis of emotion: a meta-analytic review. *Behav. Brain Sci.* **35**, 121–143 (2012).
47. Qin, P. & Northoff, G. How is our self related to midline regions and the default-mode network? *Neuroimage* **57**, 1221–1233 (2011).
48. Kable, J.W. & Glimcher, P.W. The neural correlates of subjective value during intertemporal choice. *Nat. Neurosci.* **10**, 1625–1633 (2007).
49. Laird, A.R. *et al.* Investigating the functional heterogeneity of the default mode network using coordinate-based meta-analytic modeling. *J. Neurosci.* **29**, 14496–14505 (2009).
50. Andrews-Hanna, J.R., Reidler, J.S., Sepulcre, J., Poulin, R. & Buckner, R.L. Functional-anatomic fractionation of the brain's default network. *Neuron* **65**, 550–562 (2010).

ONLINE METHODS

Participants. Nineteen participants with normal or corrected-to-normal vision took part in the study. Two participants were excluded from analysis, one because of excessive eye-movement artifact that contaminated more than 50% of the trials and the other because of extremely low heart rate (mean interbeat interval of 1.3 s compared to 0.8 s on average in other subjects). The data from 17 subjects were analyzed (eight male; two left-handed; mean age: 23.7 ± 0.5 years). All subjects signed a written informed consent and were paid for their participation. All procedures were approved by the local ethics committee (Comité de protection des personnes Ile de France III).

Stimuli. Stimuli consisted of a grating annulus (spatial frequency, five cycles per degree of visual angle; inner and outer radius, 2.5° and 3° of visual angle, respectively; orientation chosen among 20 equally spaced between 0° and 180°, with cardinal orientations (±30° around the horizontal and vertical orientations) being excluded). The fixation mark was a black dot (radius, 0.15° of visual angle) surrounded by a black circle (radius, 0.5° of visual angle) at the center of the screen. All stimuli were presented on a gray background (luminance, 4.6 cd m^{-2}) at a viewing distance of 0.8 m.

Paradigm. An experimental session consisted of six to eight blocks with 80 stimulus-present trials and 12 stimulus-absent trials interleaved randomly per block. A trial was initiated when subjects fixated on the center of the screen without saccades larger than 1.5° of visual angle for 0.5–0.7 s. The fixation mark then turned red, and after a variable delay of 1.5–1.7 s, the stimulus was presented for 50 ms in 87% of the trials. After a further variable delay of 0.3–0.7 s, subjects reported whether or not they saw the stimulus with the index and middle finger of the right hand. Response mapping was counterbalanced between subjects. The black fixation mark remained on the screen during the intertrial interval (1.5–2 s). To adjust stimulus contrast so that the hit rate would be around 50%, each experimental session began with a calibration procedure during which the participant performed the task described above. Stimulus contrast varied from trial to trial according to a one-up one-down staircase. The procedure was repeated twice, and the mean of the two thresholds obtained was used for the remainder of the experiment. At the beginning and end of the experimental session, resting-state data were acquired for 3 min while subjects fixated on the center of the screen.

Recordings. Continuous MEG signals were collected using a whole-head MEG system with 102 magnetometers and 204 planar gradiometers (Elekta Neuromag TRIUX MEG system) at a sampling rate of 1,000 Hz and online low-pass filtered at 330 Hz. 7 EKG electrodes were placed around the base of the neck and referenced to a left abdominal location. The ground electrode was located between the shoulder blades. Two EKG electrodes were placed over the left and right clavicles, two over the top of the left and right shoulders, two over the left and right supraspinatus muscle and one over the upper part of the sternum. A vertical electrooculogram (EOG) was simultaneously recorded. Horizontal and vertical eye position as well as pupil diameter were monitored using an eye tracker (EyeLink 1000, SR research) and recorded together with MEG, EKG and EOG data. Peripheral blood pressure was measured on the left thumb using the BIOPAC NIBP-MRI system, to which we added a home-mounted pressure transducer MPX5100 to directly record peripheral blood pressure in arbitrary units but in perfect time registration with the MEG and EKG data. Because of a number of technical problems, good-quality peripheral blood pressure data could be acquired in 11 subjects only.

Signal detection theory. Sensitivity (d') and criterion ($\log(\beta)$) were computed as $z(HR) - z(FAR)$ and $(z(FAR)^2 - z(HR)^2)/2$, respectively, with HR corresponding to hit rate and FAR corresponding to false alarm rate. Null false alarm rates were adjusted to $1/2N$, where N is the number of stimulus-absent trials[51]. In this case, sensitivity (and the respective criterion) computed across all trials is not identical to the mean of the sensitivities (and the respective criterion) computed on separate trial bins, and only sensitivities (and the respective criterion) computed on similar trial numbers can be compared.

Data preprocessing. Signal space separation was performed using MaxFilter to remove external noise. Data preprocessing was then performed using in-house software. Continuous MEG and EKG data were offline filtered between 1 and 40 Hz using a fourth-order Butterworth filter. Epochs contaminated with eye movements (rejection threshold, 1° of visual angle from fixation), blinks and muscular artifacts in the time window ranging from onset of the warning stimulus to 600 ms after stimulus presentation were rejected offline on the basis of eye-tracker, EOG and MEG signals, respectively. The same procedure was applied on resting sessions.

Heartbeat-evoked responses were computed on magnetometer signals locked to the T peak of the EKG. T peaks were detected in a two-step procedure. We first identified R peaks on EKG lead 2 by correlating the EKG lead 2 signal with a template QRS complex defined on a subject-by-subject basis and identified local maxima within episodes of correlation larger than 0.7. We then correlated a template of the T peak with EKG data and identified the local maximum within episodes of correlations above 0.5 that followed an R peak by at most 0.5 s. We then selected those T peaks occurring from 300 ms after the warning onset up to 400 before stimulus onset to avoid heartbeat-evoked responses being contaminated by responses to the warning or to the stimulus. We then averaged magnetometer signals from 350 ms before the T peak to 350 ms after the T peak to generate T-locked prestimulus responses to heartbeats.

Source localization. Source localization and surface visualization were performed with the BrainStorm toolbox[52]. Electrical cortical activity was estimated using a distributed model consisting of 15,000 current dipoles. Absolute values of dipole moments, in pA × m, directly quantify neural activity. Dipole orientations were constrained loosely to the cortical mantle of a generic brain model built from the standard brain model of the Montreal Neurological Institute fitted to each subject's head shape. Cortical current maps were computed from the combined time series of magnetometer and gradiometer signals using a linear inverse estimator (weighted minimum-norm current estimate) separately for each condition and for each subject. Cortical currents were then averaged over the time window in which a significant difference between hits and misses was identified in sensor space using the cluster-based permutation test. The reliability of the difference in absolute dipole current values was assessed by computing the t statistic between conditions and searching for regions containing at least ten adjacent vertices whose t value exceeded an uncorrected P value of 0.005. This approach was complemented by a cluster-based approach, as detailed below, for a more stringent correction for multiple comparisons. The anatomical description is based on the Tzourio-Mazoyer parcellation[53].

EKG analysis. In addition to the seven vertical EKG signals recorded, we offline computed the seven bipolar horizontal derivations between adjacent electrodes. This procedure was developed to estimate as best as possible the cardiac field artifact reaching the MEG sensors and control for any difference in intrinsic heart electrical activity between hits and misses. EKG measures were preprocessed in an identical manner to the MEG data. Interbeat intervals were measured between R peaks.

Independent component analysis correction. We attenuated the cardiac field artifact in the MEG data using independent component analysis (ICA) as implemented in the FieldTrip toolbox[54] in data acquired during detection and rest. ICA was applied to epoched data from 1.5 s before to 1.5 s after T peaks separately in hits and misses. We then removed all independent components with a mean 0–40 Hz coherence with EKG data larger than 0.3. 1 to 3 components were removed in each subject.

Respiratory pattern analysis. Respiration rate can be retrieved from the electrocardiogram with excellent accuracy (~98%) when subjects are resting or sitting by bandpass filtering EKG signals around breathing frequency[55]. We filtered lead 2 signals between 0.2 and 0.8 Hz (fourth-order Butterworth filter). To determine respiration period, we detected zero crossings and computed the length of the respiration cycle during which the warning stimulus occurred separately in hits and misses. To determine respiration phase, we computed the Hilbert transform to measure the respiration instantaneous phase at stimulus onset. To test for differences in phase distribution between hits and misses, we computed the phase bifurcation index, Θ (ref. 56), between hits and misses in each subject, a measure that departs from zero when phase locking differs between two conditions. The distribution of Θ under the null hypothesis was established by randomly assigning single trials the label 'hit' or 'miss' in each subject,

computing Θ and repeating the procedure 1,000 times. The original Θ value was compared against this distribution to compute the corresponding Monte-Carlo *P* value.

Blood pressure analysis. Peripheral blood pressure data were 1–40 Hz bandpass filtered (fourth-order Butterworth) and mean centered, giving rise to positive as well as negative values. Systolic pressure was measured as the peaking pressure value at each cardiac cycle, and diastolic pressure was measured as the preceding local minimum.

Statistical analyses. The significance of the difference in heartbeat-evoked responses between hits and misses was tested using the cluster-based permutation *t* test[57] as implemented in the FieldTrip toolbox[54]. This procedure extracts spatiotemporal regions showing significant differences between conditions without any a priori on spatial regions nor time windows and intrinsically corrects for multiple comparisons in space and time. Briefly, individual samples whose *t* value exceeds a threshold ($P < 0.05$, two tailed) are clustered based on temporal and spatial adjacency. Each cluster defined in time and space by this procedure is assigned cluster-level statistics corresponding to the sum of the *t* values of the samples belonging to that cluster. Type 1 error rate is controlled by evaluating the maximum cluster-level statistics under the null hypothesis: condition labels are randomly shuffled 1,000 times to estimate the distribution of maximal cluster-level statistics obtained by chance. The two-tailed Monte-Carlo *P* value corresponds to the proportion of elements in the distribution of shuffled maximal cluster-level statistics that exceeds the observed maximum or minimum original cluster-level test statistics. Because this method uses maxima, it intrinsically corrects for multiple comparisons in time and space.

This procedure was applied at the sensor level on magnetometers in the artifact-free time window (50–350 ms). The same procedure was applied at the source level on currents averaged between 135 and 171 ms across the 15,000 vertices of the cortical model. It was also used on EKG data separately for vertical and horizontal derivations, focusing on the time window before and during the difference observed at the sensor level between 50 and 171 ms after the T peak to maximize the sensitivity of the method that increases with decreasing numbers of samples.

Degrees of freedom in repeated-measure ANOVA were corrected (Greenhouse-Geisser method) for violation of the sphericity assumption when appropriate. All statistical tests were two sided.

No statistical test was run to determine sample size a priori. The sample sizes we chose are similar to those used in previous publications. Although we were not blind to the experimental conditions, the data collection and analyses were automated to avoid the introduction of bias.

51. Macmillan, N.A. & Creelman, C.D. *Detection Theory: a User's Guide* (Lawrence Erlbaum Associates, 2005).
52. Tadel, F., Baillet, S., Mosher, J.C., Pantazis, D. & Leahy, R.M. Brainstorm: a user-friendly application for MEG/EEG analysis. *Comput. Intell. Neurosci.* **2011**, 879716 (2011).
53. Tzourio-Mazoyer, N. *et al.* Automated anatomical labeling of activations in SPM using a macroscopic anatomical parcellation of the MNI MRI single-subject brain. *Neuroimage* **15**, 273–289 (2002).
54. Oostenveld, R., Fries, P., Maris, E. & Schoffelen, J.M. FieldTrip: open source software for advanced analysis of MEG, EEG, and invasive electrophysiological data. *Comput. Intell. Neurosci.* **2011**, 156869 (2011).
55. Boyle, J., Bidargaddi, N., Sarela, A. & Karunanithi, M. Automatic detection of respiration rate from ambulatory single-lead ECG. *IEEE Trans. Inf. Technol. Biomed.* **13**, 890–896 (2009).
56. Busch, N.A., Dubois, J. & VanRullen, R. The phase of ongoing EEG oscillations predicts visual perception. *J. Neurosci.* **29**, 7869–7876 (2009).
57. Maris, E. & Oostenveld, R. Nonparametric statistical testing of EEG- and MEG-data. *J. Neurosci. Methods* **164**, 177–190 (2007).

doi:10.1038/nn.3671